

## Mechanisms of Aqueous Extraction of Soybean Oil

K. A. CAMPBELL AND C. E. GLATZ\*

Department of Chemical and Biological Engineering Iowa State University Ames, Iowa 50011-2230

Aqueous extraction processing (AEP) of soy is a promising green alternative to hexane extraction processing. To improve AEP oil yields, experiments were conducted to probe the mechanisms of oil release. Microscopy of extruded soy before and after extraction with and without protease indicated that unextracted oil is sequestered in an insoluble matrix of denatured protein and is released by proteolytic digestion of this matrix. In flour from flake, unextracted oil is contained as intact oil bodies in undisrupted cells, or as coalesced oil droplets too large to pass out of the disrupted cellular matrix. Our results suggest that emulsification is an important extraction mechanism that reduces the size of these droplets and increases yield. Protease and SDS were both successful in increasing extraction yields. We propose that this is because they disrupt a viscoelastic protein film at the droplet interface, facilitating droplet disruption. An extraction model based on oil droplet coalescence and the formation of a viscoelastic film was able to fit kinetic extraction data well.

**KEYWORDS:** Aqueous processing; protein; oil; soybeans; extraction; enzyme

### INTRODUCTION

Aqueous extraction processing (AEP) of soy is a promising green alternative to hexane extraction processing. While recent advances in AEP techniques have increased the recovery of free oil to 85% (1), AEP yields are still less than typical yields from industrial hexane extraction processes. AEP uses water as an extraction medium, dissolving soluble cellular materials and allowing the release of oil into the bulk liquid phase, from which the oil can be recovered by centrifugation resulting in a cream emulsion which can be broken to recover free oil (1–3). Approximately 10–15% of the oil released from the solid fraction also remains in the aqueous fraction as an emulsion stable toward creaming (1). Because of the immiscible nature of the oil/water system, the poorly understood mechanisms of oil release are intrinsically different than those from hexane extraction processes. In order to increase yields of AEP, a thorough understanding of the extraction mechanisms is needed.

Important parameters for extraction from soy flour are pH, particle size, agitation rate, solid–liquid ratio, extraction time, and temperature (4–7). The use of protease and cellulase enzymes has also had significant effects on oil extraction yield from soy flours and extrudates in processes referred to as enzyme-assisted aqueous extraction processing (EAEP) (1, 6, 8, 9). In soy, there is an association between protein solubility and oil extraction. At pH 4.5 (the average *pI* of soy protein), where soy protein solubility is very low (<10%) (10), both protein and oil extraction yields are lower (5). Heat-abused soy flours, with likely protein denaturation, also showed reduced protein and oil yields (5); however, these yields increased with proteolysis (6). Soy protein bodies occupy most of the intracellular volume of soy

cotyledon cells (11) and, therefore, could pose a physical barrier to oil release. Additionally, soy protein may bind oil by physical entrapment in insoluble protein at oil/protein ratios up to 111–145 and 67–94 g of oil/100 g of protein for soy protein isolates and concentrates, respectively (12). In soybean, the oil–protein ratio is such that the quantity of protein present is more than enough to sequester all of the oil in an isoelectric precipitate.

Rosenthal et al. showed that oil and protein extraction yield were directly proportional to the inverse of flour particle size, which they attributed to cellular disruption enabling oil and protein release (5). They also attributed the oil yield benefits of agitation to increased cellular disruption. The immiscible nature of the AEP/EAEP systems suggests that a potential role for emulsification in the extraction mechanism should not be overlooked; agitation's effect on emulsification could be another explanation for the effect of agitation on oil extraction yield.

Oil release from a confining cellular matrix requires mobility of oil droplets within this matrix; mobility will be a function of droplet size and matrix geometry. The matrix geometry is determined by the native cellular geometry, the mode of cellular disruption used (i.e., flaking, milling, extrusion, etc.), and the solubility of the intercellular matrix. Oil droplet size is determined by stability of the oil storage organelles, i.e., oil bodies, in the extraction medium, specific energy input into the extraction medium (imparted by the agitator), and properties of the oil/water interface. While studies on oil body isolation indicate that oil bodies are stable at the temperature and pH commonly used in AEP (50 °C and pH 8–9) (13), interfacial surface proteins of cream from AEP of soy flour created at pH 8 are composed mostly of storage proteins with only minor quantities of oleosin, the primary oil body membrane protein (2). This indicates that few, if any, native oil bodies survive the extraction process, and the oil droplets may have undergone many cycles of coalescence and disruption. Droplet disruption and coalescence

\*To whom correspondence should be addressed, at Department of Chemical and Biological Engineering, 2114 Sweeney Hall, Iowa State University, Ames, IA 50011-2230. Phone: 515-294-8472. Fax: 515-294-2689. E-mail: cglatz@iastate.edu.

during turbulent mixing may also explain why Nikiforidis and Kiosseoglou observed a mixture of interfacial proteins in AEP of corn germ, which they attributed to multilayer protein adsorption on native oil bodies (14).

Emulsion particle size distribution is determined by a balance of two opposing events—droplet coalescence and droplet break-up—under the influence of dispersed phase viscosity, interfacial tension (which is affected by surfactant concentration), continuous phase density, and specific energy input. Theoretical and semiempirical models have been developed that predict maximum stable droplet size with success (15). For an inertial breakup mechanism, the maximum stable drop diameter is

$$d_D = A_1 \left( 1 + \frac{A_2 \eta_D \varepsilon^{1/3} d_D^{1/3}}{\sigma} \right) (\varepsilon^{-2/5} \sigma^{3/5} \rho_C^{-3/5}) \quad (1)$$

where  $d$  is droplet diameter,  $\eta$  is dynamic viscosity,  $\varepsilon$  is specific energy input,  $\sigma$  is interfacial tension,  $\rho$  is density, subscripts C and D denote continuous and dispersed phases, respectively, and  $A_1 \approx 1.0$  and  $A_2 \approx 3.5$  are numerical constants (15).

Soy proteins, having high surface activity, will alter the tension of an oil–water interface (16); therefore, they are important for emulsification during AEP. Emulsification properties of soy proteins have been widely studied (8, 17, 18), but interfacial rheology of the oil–water interface in the presence of soy proteins has not. Proteins are similar to low molecular weight (LMW) surfactants in that they will adsorb to an oil–water interface and reduce static surface tension. However, large proteins diffuse to and along the interface slowly compared to LMW surfactants and change conformation upon adsorption to maximize hydrophobic/hydrophilic interactions with the two different phases (19). Adsorbed proteins often exhibit strong intermolecular interactions and form a viscoelastic film, which may restrict droplet deformation (19–22) and make interfacial membranes more difficult to break (20). Oil droplets thus stabilized often exhibit properties similar to deformable capsules rather than a viscous droplet (23). Therefore, in the presence of surface active proteins, the maximum stable droplet diameter could be much larger than predicted by eq 1 from measurement of the static interfacial tension. In mixed protein/surfactant systems, LMW surfactants tend to dominate over high molecular weight polypeptides in determining interfacial rheology, primarily because of diffusion and denaturation kinetic limitations of proteins (20). However, preformed protein films can be disrupted and even displaced from an interfacial surface by sodium dodecyl sulfate (SDS) (19, 24). The currently accepted model of droplet destabilization in protein–surfactant systems shows that destabilization is maximized when there is only a partial displacement of protein at the interface such that both protein and surfactant species are immobile, while the protein network is disrupted (25).

For  $\beta$ -lactoglobulin, which has one free sulfhydryl (SH) group per molecule, disulfide bridging between interfacial proteins plays an important role in interfacial surface rheology (26) as well as in emulsion stability (27). Glycinin and  $\beta$ -conglycinin, the major storage proteins in soybean, have between 0.36 and 1.6 mol of SH per mol of protein (28, 29); therefore, interfacial polymerization could also play an important role in droplet stability for AEP emulsions. Cystine SH groups have a  $pK_a$  of 8.3. Therefore, deprotonated initiating SH groups would be readily available at AEP conditions (between pH 8 and 9); SH polymerization of  $\beta$ -lactoglobulin occurs readily at pH 7 (27, 30). Increased interfacial film elasticity impedes LMW surfactants from displacing interfacial proteins stabilized by disulfide bridging (25). Still, SDS is known to weaken  $\beta$ -lactoglobulin films at high molar ratios (19).

In this work, we observed microstructural changes by microscopy of soy disrupted by alternative mechanical methods and studied the effects of agitation rate, solid–liquid ratio, and enzyme concentration on oil extraction from the disrupted soy. Release kinetics, compartmental modeling, and microscopic observation were combined to establish a mechanistic extraction model.

## MATERIALS AND METHODS

**Materials.** Soybeans were prepared at the Iowa State University Center for Crops Utilization Research using local common variety, 2005 and 2007 harvest. Four modes of comminution were investigated: flour, flake, flour from flake, and extrudate. Flour was prepared by passing cracked dehulled soybeans twice through a pin-mill. Soy flake was prepared by passing cracked dehulled soybeans through a smooth surface roller to a thickness of approximately 0.25 mm. Flour from flake was produced by passing flakes once through a pin-mill. Extrudate was produced by extruding soy flake as described previously (1). All flours were stored at  $-20$  °C until use. Protex 7L (P7L), a neutral metallo-endoprotease from *Bacillus amyloliquefaciens*, with optimum temperature and pH ranges of 40–60 °C and 6–8, respectively, and Protex 6L (P6L), an alkaline serine-endoprotease from *Bacillus licheniformis*, optimum temperature and pH ranges 30–70 °C, and 7–10, respectively, were kindly provided by Genencor International (Rochester, NY) as a water–propylene glycol solution containing <10% protein (w/w) as received from the manufacturer.

**Flour from Flake Particle Size Distribution.** Flour from flake particle size distribution was measured by laser light scattering (Mastersizer 2000 S, Malvern Instruments, Ltd., Chicago, IL). A flour suspension was prepared by adding 1 g of flour to 175 mL of deionized water initially at pH 2.7 for a final pH of 4.5, then agitating for 3 h to break up clumps. Aliquots were introduced to the instrument by transfer pipet.

**Microscopy.** For transmission electron microscopy (TEM) and light microscopy (LM), samples were fixed and embedded following Bair and Snyder (11) with minor modifications at the Microscopy and Nanolmaging Facility at Iowa State University. Whole seed was imbibed overnight in deionized water; comminuted samples were placed directly into fixative solution. Tissues were fixed in 2% glutaraldehyde (w/v) and 2% paraformaldehyde (w/v) in 0.1 M cacodylate buffer, pH 7.2 for 48 h at 4 °C. Samples were rinsed 2 times in 0.1 M cacodylate buffer (pH 7.2) and then fixed in 1% osmium tetroxide in 0.1 M cacodylate buffer for 1 h (room temp.) The samples were then dehydrated in a graded ethanol series, cleared with ultrapure acetone, infiltrated and embedded using a spurr's epoxy resin (Electron Microscopy Sciences, Ft. Washington, PA). Resin blocks were polymerized for 48 h at 65 °C. Thick and ultrathin sections were made using a Reichert Ultracut S ultramicrotome (Leeds Precision Instruments, Minneapolis, MN). Thick sections were contrast stained using 1% toluidine blue. Ultrathin sections were collected onto copper grids and counter-stained with 5% aqueous uranyl acetate for 15 min followed by Sato's lead stain for 10 min. Images were captured using a JEOL 1200EX scanning and transmission electron microscope (Japan Electron Optic Laboratories, Peabody, MA). Light microscopy images were captured using a Zeiss Axioplan 2 light microscope (Carl Zeiss MicroImaging, Inc., Thornwood, NY).

**Extraction.** Extractions were performed in a 2 L jacketed glass reaction vessel (model 4742, Chemglass Inc., Vineland, NJ) held at 50 °C by a circulating water bath, and agitated by a stirrer (model BDC 3030, Caframo, Ltd., Warton, Ontario) with a 2 in. diameter, 3-bladed screw impeller. Constant pH of 8.0 (flour from flake) and 9.0 (extrudate) was maintained using an autotitrator (model 718 Stat Titrimo, Metrohm, Ltd., Herisau, Switzerland). For response surface extractions flour from flake was extracted in deionized water without enzyme with an agitation rate of 500 rpm for 120 min to extract as much oil as possible without enzyme. After 120 min, enzyme was added and agitation rate was changed to the test condition for an additional 120 min. All other extractions were carried out for four hours with any additions made at the start of the extraction. Extractions for flour from flake and extrudate utilized P7L and P6L, respectively. At the end of the extraction, two 35 mL samples were withdrawn by siphon from the center of the reactor. Samples were centrifuged at 3000g for 15 min. Sample fractions (solid and liquid) were massed and solid fractions were retained for analysis. Solid fraction

**Table 1.** Factor Levels Chosen for Response Surface Design Experiment for Flour from Flake<sup>a</sup>

S/L	real variables		coded variables		
	E/S	A (rpm)	S	E	A
0.050	0.5%	200	-1	-1	-1
0.010	1.0%	500	0	0	0
0.015	1.5%	1500	1	1	1

<sup>a</sup>Agitation (A) is varied logarithmically, and solid-liquid ratio (S/L) and enzyme-solid ratio (E/S) are varied linearly.

moisture content was determined by drying in an oven at 130 °C for 12–15 h. Solid fraction oil content was determined on freeze-dried samples using a Goldfish extraction apparatus (AOCS Official Method Bc 3-49). Oil and protein yields were determined based on the difference between content of the starting material and the content of the solid fraction. Protein dissolution was calculated as including the protein in the liquid fraction plus that solubilized protein entrained in the solid fraction, which was estimated by multiplying the liquid fraction protein concentration times the mass of water in the solid fraction.

**Experimental Design and Statistical Analysis.** A response surface experimental design was used to test factor effects on oil extraction yield and to develop an empirical model for process optimization. A Box-Behnken design with three center points was selected, with three factors: solid-liquid ratio (S), enzyme-solid ratio (E) and agitation rate (A). Real values and coded values are shown in **Table 1**. Statistical analysis was completed using JMP 6.0 statistical software package by SAS, Inc., Cary, NC.

**Interfacial Tension.** Interfacial tension of a soy oil/skim interface was measured by the Wilhelmy Plate method using a FACE Automatic Surface Tensiometer (Kyowa Interface Science Co. Ltd., Niiza-City, Japan). Skim was carefully poured over oil phase (Hy-Vee brand 100% soy oil, Hy-Vee, Inc., West Des Moines, IA) in a glass dish and allowed to stand for one hour to achieve interfacial equilibrium before measurement.

**Viscosity.** Viscosity was measured using a Cannon-Fenske 50 viscometer (Cannon Instrument Company, State College, PA) in a 50 °C water bath.

**Degree of Hydrolysis.** Degree of hydrolysis (DH) was estimated using the pH stat technique (10) by measuring the volume of base added to maintain constant pH according to

$$DH = \frac{VN_b}{\alpha Ph_t} \quad (2)$$

where  $V$  and  $N_b$  are the volume and normality of base added, respectively,  $\alpha$  is the fraction of deprotonated terminal protein residues (0.88 for soy protein at pH 8 and 50 °C (10)),  $P$  is the mass of protein being hydrolyzed, and  $h_t$  is the total number of peptide bonds per mass of protein (7.8 mequiv/g soy protein (10)).

## RESULTS

**Microscopic Analysis of Effects of Comminution and Extraction.** Typical soy cotyledon cells are about 30–50  $\mu\text{m}$  in diameter and 70–80  $\mu\text{m}$  long (31, 32). **Figure 1** shows a TEM of a native soybean cotyledon radial cross section. Most evident in the cross-section are the protein bodies, where about 80% of the soy protein is stored. The oil is stored in oil bodies, protein-phospholipid delimited lipid storage organelles (33) which fill most of the cytoplasmic network.

The microstructure of soybeans comminuted by four alternative methods—milling, flaking, flaking followed by milling (flour from flake), and extrusion—was studied by microscopy. Images (**Figure 2**) were selected to show the range of cellular disruption observed. Regions of intact cells were found in all samples but the extruded material, which provided practically complete cellular disruption (**Figure 2D**). The ultrastructure of disrupted cells, shown by TEM (**Figure 3**), showed a range of oil body alterations. In intact cells, oil bodies were mostly unaltered

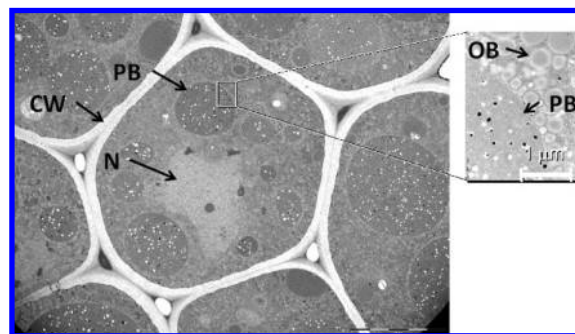


**Figure 1.** TEM of soybean cotyledon cell cross-section. PB, protein body; CW, cell wall; N, cell nucleus; OB, oil body.

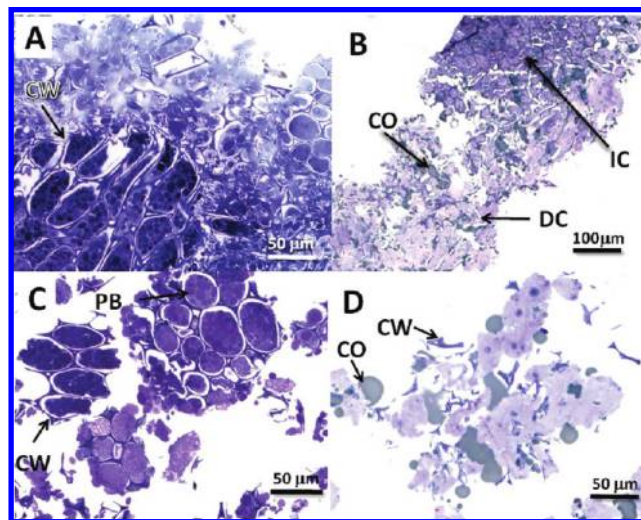


**Figure 2.** Light microscopy images of soy after various modes of comminution: (A) milling (flour); (B) flaking; (C) flaking followed by milling (flour from flake); (D) extrusion. PB, protein body; CO, coalesced oil; CW, cell wall fragment; IC, region of intact cells; DC, region of disrupted cells.

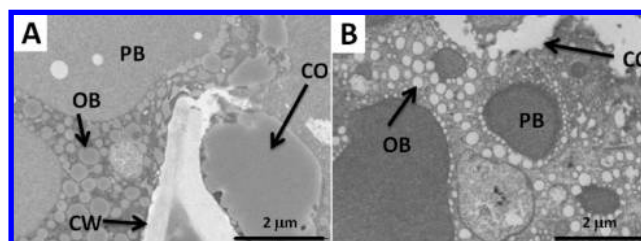


**Figure 3.** TEM of ultrastructure of (A) flour and (B) flour from flake before extraction. PB, protein body; OB, oil body; CO, coalesced oil; CW, cell wall. Osmium tetroxide stain likely did not penetrate the sample of image B, leaving the lipids with a transparent appearance.

from their pretreatment appearance. In disrupted cells, some coalescence of oil bodies was observed, but many oil bodies remained intact even in completely disrupted cells.

Images of material after two hours of AEP both with and without protease for flour from flake and extruded material are shown in **Figure 4**. In flour from flake without protease (**Figure 4A**), very little of the residual material is extracellular. Protein bodies of disrupted cells have been dissolved, while large droplets of coalesced oil are present in some cells. Structural features of cells near the center of the flour from flake particles are unaffected by the extraction. Images of extruded material (**Figure 4B**) show oil droplets within a solid matrix both before

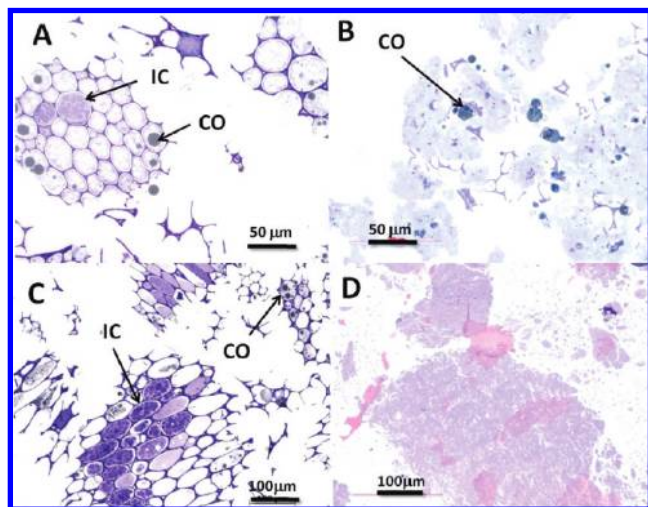


**Figure 4.** LM images of residual material after 2 h of aqueous extraction. (A) Flour from flake without protease; (B) extruded flake without protease; (C) flour from flake after two hours with 0.5% (w/w solid) Protex 7L; (D) extruded flakes after two hours with 0.5% (w/w solid) Protex 6L. CO, coalesced oil; IC, region of intact cells.

and after extraction, although the amount of oil is visibly less after extraction. The oil not extracted after two hours of AEP of extruded soy is contained within the matrix material.

For flour from flake, after two additional hours of extraction with 0.5% (w/w solid) P7L, oil extraction yield increased from 75% ( $\pm 1\%$ ) to 79% ( $\pm 1\%$ ). There was no noticeable change in the appearance of the residual flour from flake from that of the protease-free extraction (Figure 4C), possibly because only a small change in yield was achieved. It is not obvious based on these images why the addition of protease results in the increased release of oil. In the extruded material, however, the effect of protease is more pronounced, increasing yield from 68% to between 88% and 96% (1, 8). Likewise, the extracted residual is drastically altered by the addition of protease (Figure 4D). Rather than a matrix enclosing oil droplets, as seen in Figure 4B, the protease-treated residual is loose and amorphous with little entrained oil, bearing little resemblance to the starting material. Because the increase in oil extraction is accompanied by an increase in dissolved protein (1), the images suggest that the proteolysis dissolves the matrix of insoluble denatured proteins, allowing the release of entrained oil. The fact that cellulase enzymes had no effect on extraction yields of extruded soy (8) confirms complete cellular disruption and a release mechanism aided by dissolution of the denatured protein. The residual should contain cell wall remnants, but these did not show up in the fraction of material sampled. There was a coarse material observed on the bottom of the centrifuge tube, so it is likely that after being freed from the matrix, the cell walls settled fastest during centrifugation. Samples taken for microscopy were taken mostly from the upper half of the residual bed in the centrifuge tubes.

The contrast between soy extrudate and soy flour from flake in these images, the differences in initial oil extraction yield, and the effect of protease on extraction yield illustrate a key difference in extraction mechanisms for these two materials. For extrudate, even though a very high cellular disruption has been achieved, the protein solubility is reduced greatly by the heat and pressure of extrusion. Therefore, even if the cellular disruption is complete, the oil remains entrained in an insoluble matrix of extracellular denatured protein. In flour from flake the protein solubility is high, and so the primary barrier to release is the cell wall.

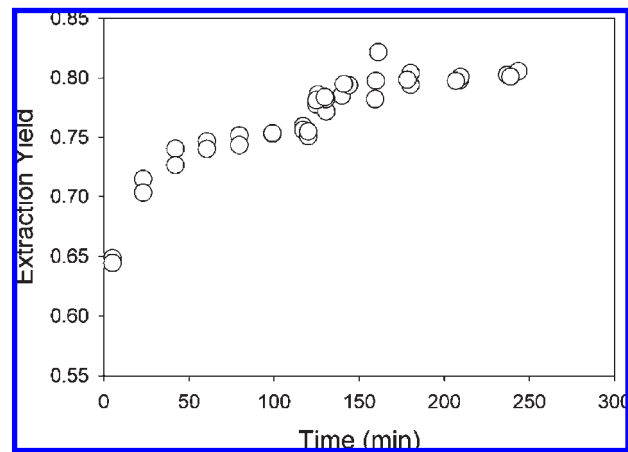


**Figure 5.** Progression of oil extraction yield for flour from flake for the response surface center-point condition: S/L = 0.10, E/S = 1.0%, and A = 500 rpm. Enzyme was added at 120 min. Data from five independent runs, two of which were up to 120 min, and three from 120 min with all five including 120 min.

**Table 2.** Significant Parameters for Oil Extraction Yield for Flour from Flake<sup>a</sup>

term	estimate	prob >  t
intercept	80.01	<0.0001
S	-5.20	<0.0001
E	0.63	0.005
A	0.49	0.017
S*E	1.30	0.001
E*E	-0.68	0.023
A*A	0.84	0.008

<sup>a</sup> Parameters studied were solid-liquid ratio (S), enzyme-solid ratio (E), and agitation rate (A) coded as shown in Table 1.

**Assessment of Significant Extraction Parameters for Flour from Flake.** The purpose of the response surface design experiment was to assess effects of enzyme-solid ratio, solid-liquid ratio, and agitation rate after nonproteolytic extraction of flour from flake had been carried out to the point of completion. Oil release before and after protease addition at the center-point conditions (S/L = 0.10, E/S = 1.0%, A = 500 rpm) is shown in Figure 5. By 120 min without protease, the extraction yield reaches a constant value of 75.3% ( $\pm 0.3\%$ ). However, when enzyme is added, oil yield increases, reaching a new maximum value of 80.0%  $\pm 0.4\%$  after an additional 120 min of extraction.

Analysis of variance of the oil extraction yield data shows that all of the parameters had significant primary effects on yield, with no significant interactions detected; values of significant effects are shown in Table 2. The model fit test is shown in Figure 6. Based on the *R*-squared value of 0.99 and randomly distributed variance, the fit appears to be very good.

Response surfaces (Figure 7) show an optimal enzyme concentration ca. 1% ( $E = 0$ ), while yield continues to increase with agitation increase and solid-liquid ratio decrease over the range tested. The small influence of agitation level between 200 and 500 rpm is probably because agitation was at 500 rpm for two hours prior to extraction. Based on microscopy and the response surface data, one concludes that the factors affecting extraction yield, in order of contribution to yield, are (1) extent of cellular disruption; (2) solid-liquid ratio; (3) enzyme-solid ratio; and (4) agitation rate. That these three parameters had significant effects on yields gives insight into possible extraction mechanisms. Agitation may increase oil extraction either by (1) disrupting the cellular matrix, thus, decreasing or widening the escape path of the oil droplets, or by (2) disrupting the oil droplets

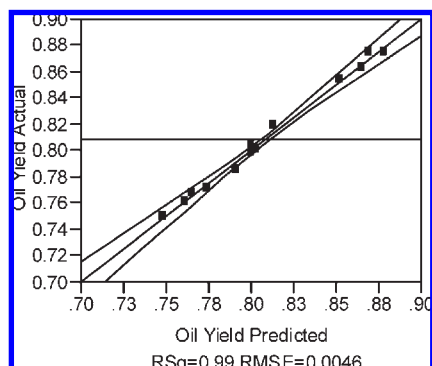


**Figure 6.** Fit test of response surface model for oil extraction yield of flour from flake with fitted parameters of **Table 2**. Points lie about a line of a slope of 1, with prediction confidence intervals shown. The horizontal line is the overall mean yield.

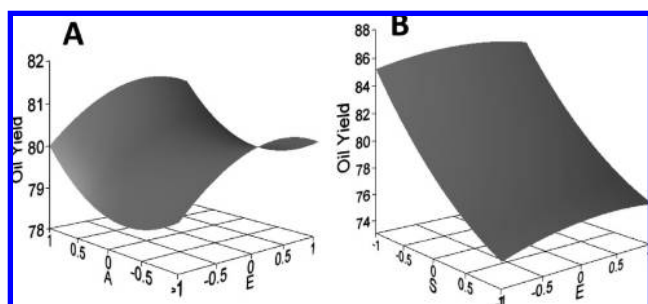


**Figure 7.** Response surfaces for oil extraction yield for flour from flake. (A) Agitation rate and enzyme concentration at a solid-liquid ratio of 0.10; (B) enzyme concentration and solid-liquid ratio at an agitation rate of 500 rpm. Agitation is varied logarithmically; solid-liquid ratio and enzyme-liquid ratio are varied linearly. Figures were generated by JMP 6.0 statistical software package.

(i.e., emulsification), easing their release from the cellular matrix. While native oil bodies are much smaller than the cellular dimensions (0.5 to 2  $\mu\text{m}$ ), microscopy of flour from flake showed that coalescence during extraction resulted in droplet sizes comparable to cell dimensions. Therefore, in order for emulsification to be an important mechanism, the power imparted by the agitator must be capable of reducing droplets to sizes small enough to affect their mobility within disrupted cells. Equation 1 provides a lower-limit estimate of this capability in the absence of viscoelastic behavior of the interface (i.e., no protein-protein interactions). Thus for the experimental value surface tension of 5 mN/m, eq 1 predicts maximum stable droplet diameters of 40  $\mu\text{m}$ , 7  $\mu\text{m}$  and 1  $\mu\text{m}$  for 200 rpm, 500 rpm, and 1500 rpm, respectively. Considering a typical cell diameter is about 30  $\mu\text{m}$ , these results show that the agitation rates used in this study do have the capability of affecting droplet mobility.

**Alteration of Interfacial Properties for Extraction from Flour from Flake.** Treatments intended to vary the interfacial composition affect extraction yield as shown in **Table 3**. Adding 3% (w/w solid) SDS increased yields by 13% compared to extraction with no additions for flour from flake. This yield increase coincided with a modest reduction in interfacial surface tension from 5.3 mN/m ( $\pm 0.2$ ) without SDS to 2.1 mN/m ( $\pm 0.1$ ) with SDS, which, according to eq 1, would have reduced the maximum stable droplet diameter from 7 to 5  $\mu\text{m}$ . It should be noted that yield without protease at S/L = 0.10 in **Table 3** is slightly lower than the pre-enzyme phase of **Figure 5**, probably because of variations among batches of flour. If the formation of a viscoelastic interfacial film by disulfide bridging or other protein-protein

interactions impede oil release from flour from flake, the addition of 3% (w/w solid) SDS appears to be successful in disrupting such a film.

While it is possible that proteolysis may increase yields by creating small polypeptides that are better emulsifiers than native proteins, this is not supported by interfacial surface tension data. The interfacial tension of skims extracted with or without protease (ca. 5 mN/m) were not significantly different (**Table 3**), suggesting a more complicated relationship between surface tension and extraction. If proteins adsorbed to the oil-water interface inhibit droplet break up by forming a viscoelastic film, then a probable mechanism through which protease affects yield is by disrupting or preventing the formation of such a protein film. Note that the difference in yields with protease (81.7%) and SDS (84.8%) is more consistent with the modest predicted reduction in droplet diameter of 7 to 5  $\mu\text{m}$  for protease and SDS, respectively.

Data in **Table 3** show that the solid-liquid ratio has no significant effect on interfacial tension, although this parameter had the largest effect on yield in the response surface experiment. If the extraction yield (and therefore droplet mobility) is an indicator of intracellular oil droplet size, then use of the static interfacial tension with eq 1 does not give an accurate description of droplet size in the absence of protease or SDS, as would be expected if viscoelastic effects were inhibiting droplet breakup. The fact that solid-liquid ratio has such a strong effect on extraction yield may support the hypothesis of protein adsorption hindering droplet breakup, thereby reducing extraction yield.

**Figure 8** shows extraction yield with and without protease for a wide range of solid-liquid ratio. As the solids content decreases, the yield increases. At a solid-liquid ratio of 0.10, the emulsion resulting from AEP has a multilayer protein interfacial layer of 14.5 mg/m<sup>2</sup> (2). Having a more dilute protein concentration in the liquid phase (i.e., at lower solid-liquid ratio) may result in decreased interfacial coverage and easier disruption.

While surface tension data do not explain why proteases increase extraction yield, the fact that SDS and solid-liquid ratio do have such a strong effect on yield indicates that interfacial phenomena and emulsification mechanisms are important in determining AEP/EAEP yields.

**Mechanistic Model for AEP of Flour from Flake.** Based on the microscopy of flour from flake and these emulsification hypotheses, several nonsequential events can be deduced to occur during aqueous extraction of flour: (1) instantaneous release of oil already outside of the cellular matrix from completely disrupted cells; (2) dissolution of protein bodies; (3) coalescence of oil bodies; (4) protein adsorption to the oil-water interface; (5) formation of a viscoelastic protein film at the oil-water interface; (6) breakup of coalesced droplets by inertial turbulent forces; (7) movement of droplets from the cellular matrix into the bulk fluid.

**Figure 9** shows a model constructed around these steps, assuming that steps (1) and (2) occur quickly. In the model,  $P_{e,i}$  is oil from cells of a high degree of disruption, which is already outside of the cellular matrix and is readily removed.  $P_1$  is small oil droplets (or intact oil bodies) from disrupted cells of the cellular matrix that can pass into the bulk medium after the protein bodies have dissolved. While this is occurring, oil in  $P_1$  coalesces into  $P_2$ , a pool of larger droplets that have a lower mobility and are more difficult to extract. At longer times, a protein film forms around droplets in  $P_2$ , such that the turbulent forces are no longer capable of breaking them into droplets of an extractable size and this oil joins an unextractable pool,  $P_u$ . Oil in undisrupted cells,  $P_{u,i}$ , remains unextractable throughout the extraction. All kinetic processes are assumed to be first order. The total extracted oil,  $P_{e,t}$  is the sum of the contributions from  $P_{e,i}$  and  $P_e$ .

**Table 3.** Oil Extraction Yield, Skim–Oil Interfacial Tensions, and Droplet Size Estimate for 4 h Extraction, 500 rpm with SDS, Enzyme, and No Additions Using Flour from Flake

condition	oil extraction yield (%)	interfacial tension of skim–oil interface (mN/m)	max stable droplet ( $\mu\text{m}$ ), from eq 1
oil–water	NA <sup>a</sup>	12.3 A <sup>b</sup>	11.2
no enzyme, S/L = 0.10	71.7 ( $\pm 1$ ) <sup>c</sup>	5.3 B,C	7.2
no enzyme, S/L = 0.15	71 <sup>d</sup>	4.2 B	6.4
no enzyme, S/L = 0.05	83.0 <sup>d</sup>	5.3 B,C	7.2
E/S = 0.5%, S/L = 0.10	81.0 <sup>d</sup>	5.3 B,C	7.1
E/S = 1.9%, S/L = 0.10	81.7 <sup>d</sup>	5.8 C	7.5
3% (w/w) SDS, S/L = 0.10	84.8 ( $\pm 0.2$ ) <sup>e</sup>	2.1 D	4.7

<sup>a</sup>Not applicable. <sup>b</sup>Letters denote significant differences (0.05 level). <sup>c</sup>95% confidence interval for multiple experimental trials. <sup>d</sup>Final value of kinetic data. <sup>e</sup>Mean  $\pm$  range for two replicate trials.

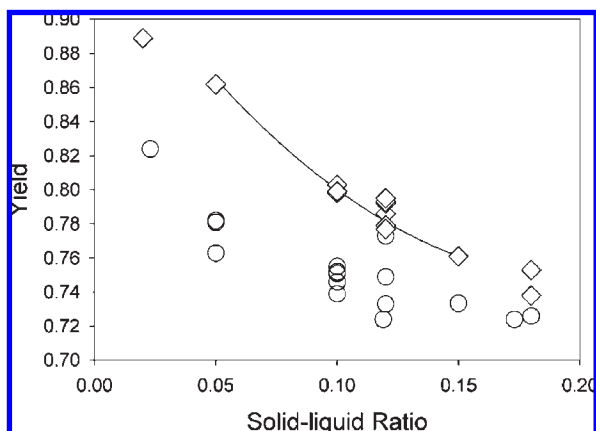


**Figure 8.** Effect of solid–liquid ratio on oil extraction yield with and without enzyme. A = 500 rpm. For enzyme extraction data, enzyme concentration ranged between 1.0% and 2.0% (w/w). Circles, yield before enzyme addition; diamonds, yield after enzyme addition; curve, response surface model for enzyme addition.

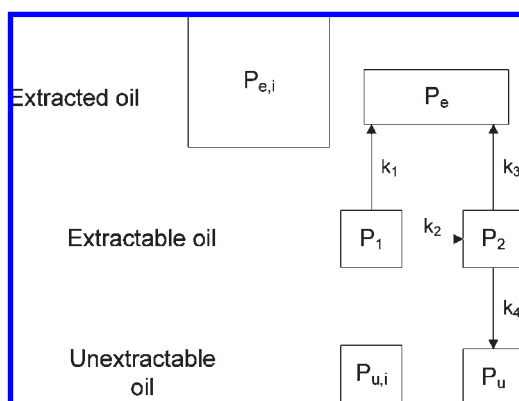


**Figure 9.** Oil extraction compartmental kinetic model for flour from flake.  $P_{e,i}$  is oil from completely disrupted cells;  $P_1$  is a pool of small oil droplets extracted quickly,  $P_2$  is coalesced oil that is extracted slowly;  $P_u$  is unextractable oil;  $P_{u,i}$  is unextractable oil contained within intact cells. All of the oil is initially contained within compartments  $P_{e,i}$ ,  $P_1$ , and  $P_{u,i}$ . As extraction progresses, oil in  $P_1$  is either extracted or coalesces into large oil droplets, represented by  $P_2$ . Larger oil droplets may be released by emulsification, however the formation of a viscoelastic protein film around oil droplets prevents this and renders the oil droplets unextractable, represented by compartment  $P_u$ .

The governing rate expressions (complete derivation provided as Supporting Information) are

$$\frac{dP_e}{dt} = -k_1 P_1 - k_3 P_2 \quad (3)$$

$$-\frac{dP_1}{dt} = (k_1 + k_2) P_1 \quad (4)$$

$$-\frac{dP_2}{dt} = -k_2 P_1 + (k_3 + k_4) P_2 \quad (5)$$

with initial conditions of  $P_e = 0$ ,  $P_1 = P_{1,o}$ ,  $P_2 = 0$ , and  $P_u = 0$  and the overall mass balance

$$1 = P_{e,i} + P_e + P_1 + P_2 + P_u + P_{u,i} \quad (6)$$

Solving these gives the expression for total oil extraction

$$P_{e,t} = P_{e,i} + P_{1,o} \left[ \left( -\frac{k_1}{K_1} - \frac{k_3 k_2}{K_1 (K_2 - K_1)} \right) (e^{-K_1 t} - 1) + \frac{k_3 k_2}{K_2 (K_2 - K_1)} (e^{-K_2 t} - 1) \right] \quad (7)$$

where  $K_1 = k_1 + k_2$ , and  $K_2 = k_3 + k_4$ .

The sizes of pools  $P_{e,i}$ ,  $P_{1,o}$ , and  $P_{u,i}$  can be estimated using particle size distribution data.  $P_{u,i}$  represents completely intact cells, which, according to microscopy of flour from flake, must reside at the center of flour particles large enough to contain intact cells. The diameter of the intact core of a flour particle will be some average length smaller than the particle itself. The fraction of total volume occupied by intact cells will therefore be

$$I = \sum_{i=55}^n F_i \left( \frac{V_{I,i}}{V_i} \right) \quad (8)$$

for all  $V_{I,i}$  greater than the average cell volume, where  $I$  is the volume fraction occupied by intact cells,  $F_i$  is the volume fraction of particles of size  $i$  as determined from light scattering analysis,  $V_{I,i}$  is the volume of the intact core of particles of size  $i$ , and  $V_i$  is the volume of particles of size  $i$ . The average dimensional length of a soy cell is approximately  $55 \mu\text{m}$  (recall that typical cellular dimensions were  $30 \mu\text{m}$  by  $80 \mu\text{m}$ ). Assuming spherical geometry for flour particles, the intact cellular core of a flour particle must have a radius about  $55 \mu\text{m}$  smaller than the particle radius, and therefore

$$V_{I,i} = \frac{4}{3} \pi (r_i - 55 \mu\text{m})^3 \quad (9)$$

where  $r_i$  is the radius of particle size  $i$ . Using the flour from flake particle size distribution with eqs 8 and 9 gives a total intact cellular fractional volume of about 4.3% of total flour volume. This agrees very well with protein extraction data with this material. Average protein extraction yields ranged from 93% ( $\pm 0.5\%$ ) without protease to 95% ( $\pm 0.7\%$ ) with protease, indicating that no more than 5% of the cells remained intact. Likewise, the fraction of oil in cells of a high degree of disruption, i.e., oil in particles less than the average cellular dimension, can be found with the cumulative size distribution function, shown in **Figure 10**. About 57% of total flour volume is made up of particles smaller than  $55 \mu\text{m}$ , suggesting that the size of pool  $P_{e,i}$  should be near 0.57. By mass balance, the fraction of total oil in cells of a partial disruption, i.e.  $P_{1,o}$ , must be near 0.38. Because

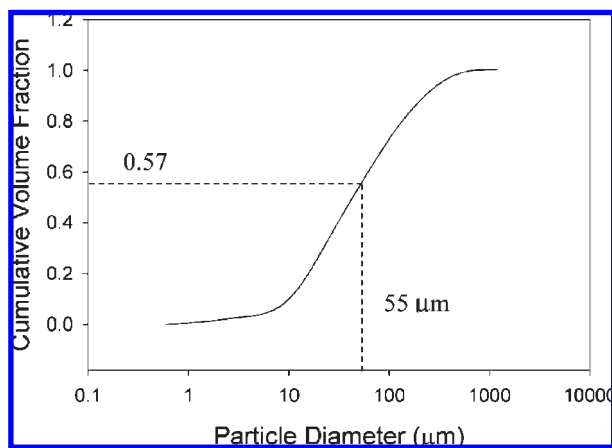


**Figure 10.** Cumulative particle size distribution (by volume) of flour from flake particles. Value shown is the volume fraction smaller than the average cellular size ( $P_{e,i}$ ) of  $55 \mu\text{m}$ .

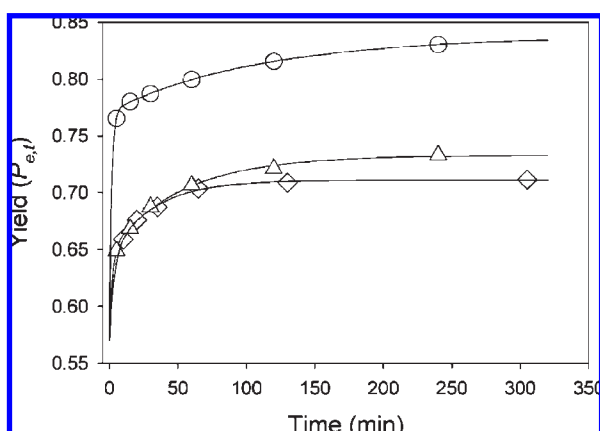


**Figure 11.** Kinetics of oil extraction for flour from flake with model fit for three different solid-liquid ratios. All extractions were without enzyme, with an agitation rate of 500 rpm. Curves represent model (eq 7) using parameters in **Table 4**. Circles,  $S/L = 0.05$ ; triangles,  $S/L = 0.10$ ; diamonds,  $S/L = 0.19$ .

the pools  $P_{e,i}$  and  $P_{1,0}$  are independent of any extraction condition (N.B. the pools would depend on the type of comminution), there are only four variable fitting parameters ( $k_1$ ,  $k_2$ ,  $k_3$ , and  $k_4$ ) to use to fit kinetic data for all extraction conditions.

Equation 7 and initial pool sizes from the particle size distribution gave good fits to kinetic extraction data, shown in **Figures 11** and **12**, with resulting parameter values shown in **Table 4**. In all cases, the value of  $k_1$ , the kinetic parameter for small droplet extraction, was at least an order of magnitude greater than  $k_3$ , the parameter for coalesced oil extraction, consistent with the model concepts where coalesced oil has a lower mobility within the cellular matrix than small droplets. For extraction without enzyme, values for  $k_2$ ,  $k_3$ , and  $k_4$  were roughly invariant with extraction conditions. This indicates that the shapes of the extraction curves are approximately the same after the first five minutes of extraction, regardless of solid-liquid ratio, and that the final yield is determined mostly by the rate of oil release in the first minutes of extraction, represented by the  $k_1$  term. Indeed, the value of  $k_1$  is enough greater for the  $S/L = 0.05$  condition that the conversion to  $P_2$  is less significant. A strategy of increasing yield by reducing the flow to  $P_2$  (and subsequently  $P_u$ ) would be to prevent coalescence. Other investigators have made recent advances in preventing oil body coalescence by extracting in sucrose, with yields similar to extraction with SDS, and very little

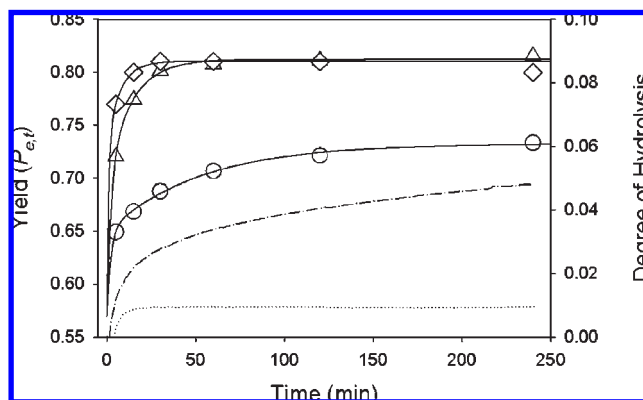


**Figure 12.** Kinetics of oil extraction yield and degree of hydrolysis for flour from flake with and without protease at a solid-liquid ratio of 0.10, and an agitation rate of 500 rpm. Solid curves represent model (eq 7) using parameters in **Table 4**. Circles, no enzyme; triangles,  $E/S = 0.5\%$ ; diamonds,  $E/S = 1.9\%$ ; dotted curve, degree of hydrolysis for  $E/S = 0.5\%$ ; dotted-dashed curve, degree of hydrolysis for  $E/S = 1.9\%$ .

oil in the skim fraction (34). The use of LMW surfactants may also prevent both coalescence and film formation and may produce an emulsion that is less stable toward creaming.

In these experiments, conversion to  $P_2$  becomes significant after ca. five minutes. To get an idea of the significance of this time scale we can compare the range of times that would be required for diffusive release of an oil body ( $0.5 \mu\text{m}$  in diameter) from a cell interior (ca.  $55 \mu\text{m}$ ). Viscosity would be the primary determinant of diffusivity. The Stokes-Einstein equation can be used to estimate diffusivity for the measured viscosity at  $S/L = 0.10$  (1.22 cP) compared to a lower limit as  $S/L$  decreases (i.e., water at 0.56 cP) which gives a time for 95% removal of 13 min vs 6 min and grows to 27 vs 13 min if the path length is the full length of a cell ( $80 \mu\text{m}$ ) (35). Hence, within the range of expected viscosities, the competing coalescence event becomes increasingly important. This also reinforces the validity of viewing  $k_1$  in terms of mass transfer.

The alternative of protein dissolution rate determining  $k_1$  seems less consistent with the time scales observed. Although collecting reproducible data on time scales much less than five minutes was not possible, the fraction of protein dissolved was already at 92.4%, within 1% of the final value (93.5%) at five minutes ( $S/L = 0.10$ ).

With one exception, the addition of enzyme increased the rates of all the processes in this model. These effects can be explained in terms of the proteolytic action. Hydrolysis may increase the rate of release of small oil droplets ( $k_1$ ) by either decreasing liquid viscosity or by increasing the rate of dissolution of protein bodies, as discussed above. However, **Figure 12** shows that the protease has the largest effect on extraction at short extraction times (less than 30 min) while the degree of hydrolysis is still very low (less than 2%). This may indicate that the effect of hydrolysis is to create small polypeptide fragments that behave like LMW surfactants, such as SDS, and assist extraction at short extraction times. Large polypeptides may have a stronger influence on droplet interfacial behavior at longer extraction times after droplets have undergone multiple cycles of breakup and coalescence, leading to similar interfacial tension measurements seen in **Table 3**. **Figure 12** also illustrates an advantage of EAEP of soy flours over soy extrudates in that increases in yields can be achieved with minimal protein alteration, leaving open the possibility of creating soy protein isolates with similar functional properties as conventional isolates.

In terms of the other mechanisms discussed, hydrolysis may increase the rate of droplet coalescence ( $k_2$ ) by disrupting the

**Table 4.** Parameter Estimates of Nonlinear Regression Fits of Eq 7 to Oil Extraction Kinetic Data for Various Solid to Liquid Ratios (S/L) and Enzyme to Solid Ratios (E/S) for Extraction from Flour from Flake<sup>a</sup>

parameter	S/L = 0.05 (no enzyme)	S/L = 0.10 (no enzyme)	S/L = 0.10 Rep (no enzyme)	S/L = 0.15 (no enzyme)	S/L = 0.15 Rep (no enzyme)	S/L = 0.19 (no enzyme)	S/L = 0.10 (E/S = 0.5%)	S/L = 0.10 (E/S = 1.9%)
$k_1$	0.331	0.059	0.101	0.018	0.022	0.064	0.170	0.500
$k_2$	0.290	0.307	0.361	0.042	0.103	0.233	0.258	0.611
$k_3$	0.003	0.006	0.005	0.001	0.004	0.006	0.029	0.046
$k_4$	0.006	0.019	0.014	0.006	0.014	0.025	0.044	0.092

<sup>a</sup> Values for  $P_{e,i}$  and  $P_{1,o}$  were 0.57 and 0.38, respectively.

oleosin membrane of the oil bodies. The release of larger coalesced oil droplets ( $k_3$ ) may also be increased if those droplets are more easily disrupted again into smaller droplets (i.e., they have a smaller maximum stable droplet diameter), which may occur if hydrolyzed proteins form weaker interfacial films. Finally, the formation of these films ( $k_4$ ) may also occur more quickly with protein hydrolyzates because smaller polypeptides would be able to diffuse more quickly to the interface than native proteins, and, because of the denaturation that occurs as a result of hydrolysis, no additional conformational changes would be necessary for intermolecular interactions to occur between polypeptides. It was also hypothesized above that the effect of enzyme may be to disrupt or prevent the formation of interfacial protein films, a state represented by  $P_u$ . However, forcing a very small value of  $k_4$  in the model resulted in noticeably poorer fits (data not shown).

In summary, the extraction model based on microscopic observation, inferences of the interfacial properties, and pool sizes predicted by particle size distribution analysis fit the experimental data well. Observed initial extraction rates are consistent with diffusion-limited extraction rates. Hydrolysis data indicate that the role of proteolysis in flour from flake extraction may be to create small polypeptides that behave similarly to a LMW surfactant.

#### ACKNOWLEDGMENT

We would like to thank Tracey Pepper and Randall DenAdel for the microscopy, Prof. Tong Wang for use of her surface tensiometer, and Peter Bierschbach of Genencor, Intl, Julia Nobrega de Moura, and the Iowa State University Center for Crops Utilization Research for providing materials used for this research.

**Supporting Information Available:** Equation derivation as noted in the text. This material is available free of charge via the Internet at <http://pubs.acs.org>.

#### LITERATURE CITED

- Moura, J.; Campbell, K.; Mahfuz, A.; Jung, S.; Glatz, C. E.; Johnson, L. Enzyme-assisted aqueous extraction of oil and protein from soybeans and cream de-emulsification. *J. Am. Oil Chem. Soc.* **2008**, *85* (10), 985–995.
- Chabrand, R. M.; Kim, H. J.; Zhang, C.; Glatz, C. E.; Jung, S. Destabilization of the emulsion formed during aqueous extraction of soybean oil. *J. Am. Oil Chem. Soc.* **2008**, *85* (4), 383–390.
- Chabrand, R. M.; Glatz, C. E. Destabilization of the emulsion formed during the enzyme-assisted aqueous extraction of oil from soybean flour. *Enzyme Microb. Technol.* **2009**, *45* (1), 28–35.
- Lusas, E. W.; Lawhon, J. T.; Rhee, K. C. Producing edible oil and protein from oilseeds by aqueous processing. *Oil Mill Gazette* **1982**, *4*, 28–34.
- Rosenthal, A.; Pyle, D. L.; Niranjan, K. Simultaneous aqueous extraction of oil and protein from soybean: mechanisms for process design. *Food Bioprod. Process.* **1998**, *76*, 224–230.
- Rosenthal, A.; Pyle, D. L.; Niranjan, K.; Gilmore, S.; Trinca, L. Combined effect of operational variables and enzyme activity on aqueous enzymatic extraction of oil and protein from soybean. *Enzyme Microb. Technol.* **2001**, *28*, 499–509.
- Rosenthal, A.; Pyle, D. L.; Niranjan, K. Aqueous and enzymatic processes for edible oil extraction. *Enzyme Microb. Technol.* **1996**, *19*, 403–429.
- Lamsal, B. P.; Murphy, P. A.; Johnson, L. A. Flaking and extrusion as mechanical treatments for enzyme-assisted aqueous extraction of oil from soybeans. *J. Am. Oil Chem. Soc.* **2006**, *83* (11), 973–979.
- Freitas, P. S.; Couri, L.; Janklonka, F.; Carvalho, C. The combined application of extrusion and enzymatic technology for extraction of soybean oil. *Fett/Lipid* **1997**, *9*, 333–337.
- Adler-Nissen, J. *Enzymatic hydrolysis of food proteins*; Elsevier Applied Science Publishers: New York, NY, 1985.
- Bair, C. W.; Snyder, H. E. Electron-Microscopy of Soybean Lipid Bodies. *J. Am. Oil Chem. Soc.* **1980**, *57* (9), 279–282.
- Nielsen, N. C. In *New Protein Foods Vol. 5: Seed Storage Proteins*; Altschul, A. A., Wilcke, H. L., Eds.; 1985; Vol. 5.
- Iwanaga, D.; Gray, D. A.; Fisk, I. D.; Decker, E. A.; Weiss, J.; McClements, D. J. Extraction and characterization of oil bodies from soy beans: A natural source of pre-emulsified soybean oil. *J. Agric. Food Chem.* **2007**, *55* (21), 8711–8716.
- Nikiforidis, C. V.; Kiosseoglou, V. Aqueous Extraction of Oil Bodies from Maize Germ (*Zea mays*) and Characterization of the Resulting Natural Oil-in-Water Emulsion. *J. Agric. Food Chem.* **2009**, *57* (12), 5591.
- Vankova, N.; Tcholakova, S.; Denkov, N. D.; Ivanov, I. B.; Vulchev, V. D.; Danner, T. Emulsification in turbulent flow: 1. Mean and maximum drop diameters in inertial and viscous regimes. *J. Colloid Interface Sci.* **2007**, *312* (2), 363–380.
- Hettiarachchy, N. In *Soybeans: Chemistry, Technology, and Utilization*, Liu, K., Ed.; Chapman & Hall: New York, 1997; p 397.
- Jung, S.; Lamsal, B.; Stepian, V.; Johnson, L.; Murphy, P. Functionality of soy protein produced by enzyme-assisted extraction. *J. Am. Oil Chem. Soc.* **2006**, *83* (1), 71–78.
- Moure, A.; Sineiro, J.; Dominguez, H.; Parajo, J. C. Functionality of oilseed protein products: A review. *Food Res. Int.* **2006**, *39* (9), 945–963.
- Mackie, A.; Wilde, P. The role of interactions in defining the structure of mixed protein-surfactant interfaces. *Adv. Colloid Interface Sci.* **2005**, *117* (1–3), 3–13.
- McClements, D. J. Protein-stabilized emulsions. *Curr. Opin. Colloid Interface Sci.* **2004**, *9* (5), 305–313.
- Fischer, P.; Erni, P. Emulsion drops in external flow fields - The role of liquid interfaces. *Curr. Opin. Colloid Interface Sci.* **2007**, *12* (4–5), 196–205.
- A. Bos, M.; van Vliet, T. Interfacial rheological properties of adsorbed protein layers and surfactants: a review. *Adv. Colloid Interface Sci.* **2001**, *91* (3), 437–471.
- Jones, D. B.; Middelberg, A. P. J. Interfacial protein networks and their impact on droplet breakup. *AIChE J.* **2003**, *49* (6), 1533–1541.
- Gunning, P. A.; Mackie, A. R.; Gunning, A. P.; Wilde, P. J.; Woodward, N. C.; Morris, V. J. The effect of surfactant type on protein displacement from the air-water interface. *Food Hydrocolloids* **2004**, *18* (3), 509–515.
- Wilde, P.; Mackie, A.; Husband, F.; Gunning, P.; Morris, V. Proteins and emulsifiers at liquid interfaces. *Adv. Colloid Interface Sci.* **2004**, *108*, 63–71.
- Bos, M. A.; van Vliet, T. Interfacial rheological properties of adsorbed protein layers and surfactants: a review. *Adv. Colloid Interface Sci.* **2001**, *91* (3), 437–471.

- (27) Damodaran, S.; Anand, K. Sulfhydryl-disulfide interchange-induced interparticle protein polymerization in whey protein-stabilized emulsions and its relation to emulsion stability. *J. Agric. Food Chem.* **1997**, *45* (10), 3813–3820.
- (28) Wu, S. W.; Murphy, P. A.; Johnson, L. A.; Fratzke, A. R.; Reuber, M. A. Pilot-plant fractionation of soybean glycinin and beta-conglycinin. *J. Am. Oil Chem. Soc.* **1999**, *76* (3), 285–293.
- (29) Wolf, W. J. Sulfhydryl content of glycinin—effect of reducing agents. *J. Agric. Food Chem.* **1993**, *41* (2), 168–176.
- (30) Kim, H. J.; Decker, E. A.; McClements, D. J. Impact of protein surface denaturation on droplet flocculation in hexadecane oil-in-water emulsions stabilized by beta-lactoglobulin. *J. Agric. Food Chem.* **2002**, *50* (24), 7131–7137.
- (31) Wolf, W. J.; Baker, F. L. Scanning Electron-Microscopy of Soybeans. *Cereal Sci. Today* **1972**, *17* (5), 124–7.
- (32) Bair, C. W. *Microscopy of soybean seeds: Cellular and subcellular structure during germination, development, and processing with emphasis on lipid bodies*. Ph.D. Thesis, Iowa State University, Ames, IA, **1979**.
- (33) Tzen, J. T. C.; Cao, Y.-s.; Laurant, P.; Ratnayake, C.; Hagenmaier, R. D. Lipids, proteins, and structure of seed oil bodies from diverse species. *Plant Physiol.* **1993**, *101*, 267–276.
- (34) Kapchie, V. N.; Wei, D.; Hauck, C.; Murphy, P. A. Enzyme-assisted aqueous extraction of oleosomes from Soybeans (*Glycine max*). *J. Agric. Food Chem.* **2008**, *56* (5), 1766–1771.
- (35) Bird, B. R.; Stewart, W. E.; Lightfoot, E. N. *Transport Phenomena*, 1st ed.; John Wiley and Sons: New York, 1960.

---

Received for review July 3, 2009. Revised manuscript received September 18, 2009. Accepted September 27, 2009. This work was sponsored by the USDA CREES Grant No. 2005-34432-1406 and 2006-34432-17128, with additional funding from the Iowa State University Plant Science Institute.